Heat Transfer 1998, Proceedings of 11th IHTC, Vol. 2
August 23-28, 1998, Kyongju, Korea

FLOW PATTERNS AND HEAT TRANSFER COEFFICIENTS IN FLOW-BOILING AND CONVECTIVE CONDENSATION OF R22 INSIDE A MICROFIN TUBE OF NEW DESIGN

Adriano Muzzio, Alfonso Niro and Marcello Garavaglia
Dipartimento di Energetica,
Politecnico di Milano
piazza Leonardo da Vinci, 32
20133 Milano
Italy

ABSTRACT

Saturated flow boiling and convective condensation experiments for oil-free refrigerant R22 have been carried out with a microfin tube of new design and with a smooth tube. Both tubes have the same outer diameter of 9.52 mm and are horizontally operated. Two-phase flow pattern data have been obtained in addition to heat transfer coefficients and pressure drops; moreover, adiabatic tests have been also performed in order for flow pattern map to cover even the adiabatic flows. Data are for mass fluxes ranging from about 90 to 400 kg/s m^2. In boiling tests, the nominal saturation temperature is 5 °C, with inlet quality varying from 0.2 to 0.6 and the quality change ranging from 0.1 to 0.5. In condensation, results are for saturation temperature equal to 35 °C, with inlet quality between 0.8 and 0.4, and quality change within 0.6 and 0.2. The comparison shows a large heat transfer augmentation with a moderate increment of pressure drops, especially in evaporation where the enhancement factor comes up to 4 while the penalty factor is about 1.4 at the most. Heat transfer coefficients both in evaporation and condensation are compared to the predictions of some recent correlations specifically proposed or modified for microfin tubes.

INTRODUCTION

Heat transfer characteristics of microfin tubes have been extensively studied over the past 18 years; detailed literature reviews are presented by (Webb, 1994), (Thome, 1994) and (Kandlikar, 1996). However, in spite of the number of published studies, there is a large demand of further experimental research in order to test new microfin tubes and refrigerants. Indeed, reliable predictions of heat transfer characteristics are experimental because of the complexity of fluid-dynamic and heat transfer processes involved. Finally, an accurate modelling and a trustworthy evaluation of heat transfer characteristics require precise predictions of the local two-phase flow patterns, since distinct flow regimes can be characterised by quite different heat transfer mechanisms. Although numerous flow pattern maps have been developed for adiabatic two-phase flows in tubes, few diabatic flow regime charts are available for flow boiling and convective condensation; while authors do not known maps for microfin tubes, except that proposed by (Manwell and Bergles, 1990).

Moved by these reasons, we are currently performing an experimental investigation of flow boiling and convective condensation of halo-carbon refrigerants inside microfin tubes as described in (Muzzio et al., 1998). This paper reports on flow patterns and average heat transfer coefficients during evaporation and condensation of oil-free refrigerant R22 in a microfin tube with a new cross-section profile, and in a smooth tube. Both tubes have the same outer diameter of 9.52 mm and are horizontally operated. In addition, adiabatic tests were also performed in order for flow pattern map to cover even the adiabatic flows. Finally, we discuss several comparisons between our experimental results and the predictions obtained both by flow pattern maps and by some recent correlations specifically proposed for microfin tubes.

EXPERIMENT

The experimental apparatus consists of three circuits, namely, a sealed refrigerant circuit, a water circuit to heat or cool the refrigerant in the test section, and a chilled coolant (water-glycol solution) circuit. A description of the apparatus is reported in (Muzzio et al., 1998). The test section is a straight, 9.52 mm o.d., copper tube that is divided in two identical, 1.3 m long, subsections. At the exit of both subsections there is mounted a sight glass made of 80 mm long, 8.5 mm i.d., pyrex smooth tube. These sight glasses are neither heated or cooled. Two pressure-taps are located at the inlet and outlet of the first subsection and at the outlet of the second one, respectively. Both subsections are equipped with four T-type thermocouples to measure wall temperatures, which are placed in pairs at 140 mm from either ends; in each pair, the thermocouples are 180 degrees apart. The thermocouples are cemented in longitudinal grooves cut in the outside wall of the tube. Every subsection is enclosed in a jacket where the heating, or cooling, water is circulated. The distance between the inlet and discharge ducts of the jacket is 1.12 m which is assumed as the active heat transfer length for the subsection. Calming and test sections are thermally insulated by a 10 cm thick, glass-wool annulus.

Signals from thermocouples and transducers are cyclically

read by a data acquisition unit and sent to an on-line PC. In order for all variables to be affected by similar RMS relative errors, the measurements of refrigerant temperature, pressure drop and water flow rate are based on 30, 50 and 100 readings for cycle, respectively. Every experimental data, instead, is obtained by averaging the measurements of ten cycles in order to reduce the influence of random errors and fluctuations. Finally, for every operative condition, ten experimental data are collected, whereas flow patterns were recorded from direct visual observations and, in some instances, videotaped.

The heat transfer coefficient is computed as follows. We assume the refrigerant temperature varies linearly between the value T_{in}, measured at the entrance of the test section, and the value T_{out} computed at the exit as $\tilde{T}_s(\tilde{p}_s(T_{in}) - \Delta p)$, where $\tilde{T}_s$ is the function correlating the saturation temperature to the pressure, $\tilde{p}_s$ the inverse function of $\tilde{T}_s$, and Δp the pressure drop measured along the test section. Then, for each subsection we calculate the mean refrigerant temperature $T_{r,m,i}$, the mean wall temperature $T_{w,m,i}$, the refrigerant to wall temperature mean difference $\Delta T_{m,i}=(T_{w,m,i}-T_{r,m,i})$, the heat flux q_i based on the subsection nominal inside area, and the heat transfer coefficient $h_i=q_i/\Delta T_{m,i}$. Eventually, we compute the average heat transfer coefficient for the test section as the arithmetic mean of the subsection coefficients h_i. Relevant variables for the present investigation are affected by the following experimental uncertainties measured or estimated by a propagation error analysis: ±2.8% for the refrigerant mass flow rate, ±1.3% for the inlet quality, ±0.2 K between the refrigerant temperature and the saturation one, ±0.03 K between the wall and refrigerant temperatures with the refrigerant trapped in the test section and the water flowing, ±1.0% for the refrigerant pressure drop, ±1.0% for the water volume flow rate, ±0.02 K for the water temperature difference between the subsection inlet and outlet, ±1.4% for the heat rate, and ±7% for the average heat transfer coefficient.

RESULTS AND DISCUSSION

In saturated flow boiling as well as in convective condensation, the average heat transfer coefficient and the pressure drop depend on four independent variables, namely, mass flux, temperature, inlet thermodynamic quality and average heat rate provided we fixed the test section geometry, i.e., cross-section profile, dimensions, and orientation with respect to gravity. In the previous list of independent variables, average heat rate can be substituted with quality change along the test section because of their linear dependence. The experimental data reported here were obtained on the microfin tube Metofin® 952-30VA40/54A, manufactured by Trefimetaux, and on a smooth tube, as well. A drawing of the cross-section profile of the microfin tube VA is reported in Fig. 1, whereas values of its geometric parameters are listed in Tab. 1 together with those of the smooth tube. This table also lists the total heat transfer internal surface ratio and the actual cross-section ratio with respect to the smooth tube. As it can be seen in Fig. 1, fins are characterised by a sharp shape and by two different heights, that is the feature distinguishing the tube VA from other microfin tubes of new design like, for example, the Hitachi Thermofin-HEX™.

Evaporation tests were carried out at a nominal saturation tem

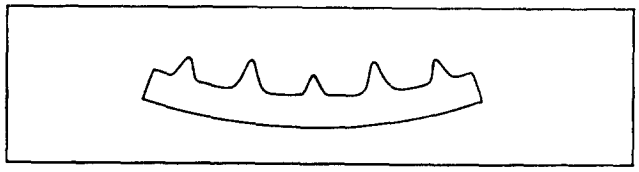

Figure 1. Drawing of the microfin cross-section profile.

Parameter	Tube	VA	Smooth
Outside diameter	(mm)	9.52	9.52
Maximum inside diameter	(mm)	8.92	8.92
Bottom wall thickness	(mm)	0.30	0.30
Higher fin height	(mm)	0.23	-
Lower fin height	(mm)	0.16	-
Apex angle		40°	-
Number of grooves		54	-
Helix angle		18°	-
Total heat transfer internal surface ratio		1.51	1
Actual cross section surface ratio		0.963	1

Table 1. Geometrical parameters of the tested tubes.

perature of 5 °C (±0.2 K) corresponding to a pressure of 0.58 MPa, while in condensation the nominal temperature was 35 °C (±0.2 K) corresponding to a pressure of 1.35 MPa. Having fixed the test temperature, three independent variables survive, namely, the mass flux, the inlet thermodynamic quality and the quality change. The mass flux G ranged from about 90 to 400 kg/s m^2 and the quality change Δx from 0.1 to 0.6; the inlet quality x_{in} was varied between 0.2 and 0.6 in evaporation, and between 0.8 and 0.4 in condensation. In addition, adiabatic tests were also performed in order for flow pattern map to cover even the adiabatic flows; these tests were carried out at a saturation temperature of 20 °C corresponding to a pressure of 0.91 MPa, within the same range of mass flux but with inlet quality between 0.05 and 0.8.

Fig. 2 shows the flow pattern data for adiabatic flow in the smooth tube, plotted on a graph where the axes represent the superficial velocities of the liquid and vapor phases, defined as $U_{ls}=G(1-x)/\rho_l$ and $U_{gs}=Gx/\rho_g$, respectively. A linear-linear format was adopted instead of the most usual log-log format, since our data have a limited range of values. Alternatively, data could be plotted using the quality and the mass flux as coordinates, as reported by (Hashizume, 1983) or by (Zürcher et al., 1997), to simplify the flow pattern identification; however, comparisons of our data to other maps should have

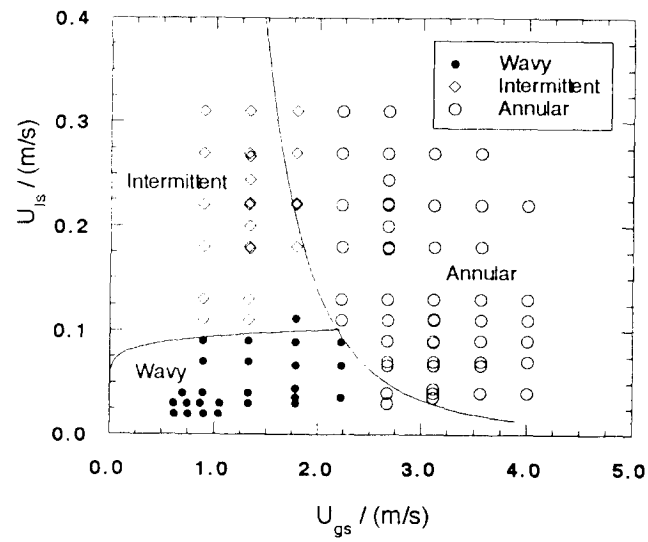

Figure 2. Flow pattern data for adiabatic flow inside the smooth tube plotted on a U_{gs}-U_{ls} graph together with the transition frontiers proposed by Weisman et al. (1979).

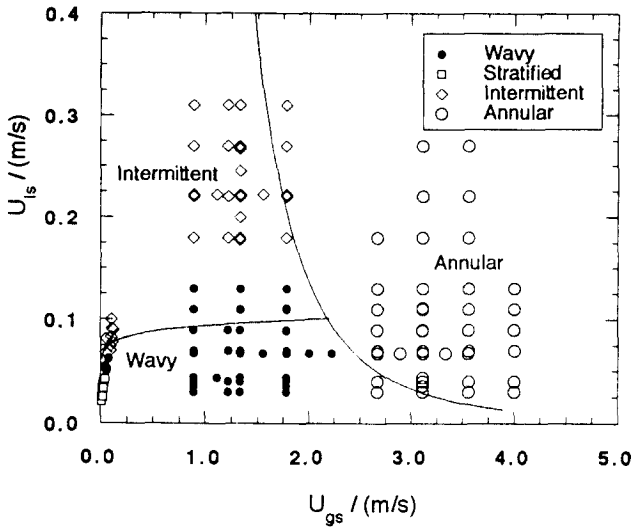

Figure 3. Flow pattern data for adiabatic flow inside the microfin tube plotted on a U_{gs}-U_{ls} graph together with the transition frontiers proposed by Weisman (1979) for smooth tubes.

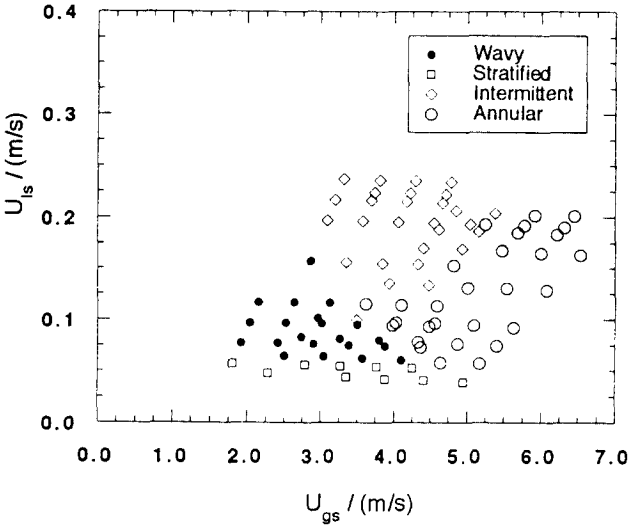

Figure 4. Flow pattern data for boiling flow inside the microfin tube plotted on a U_{gs}-U_{ls} graph.

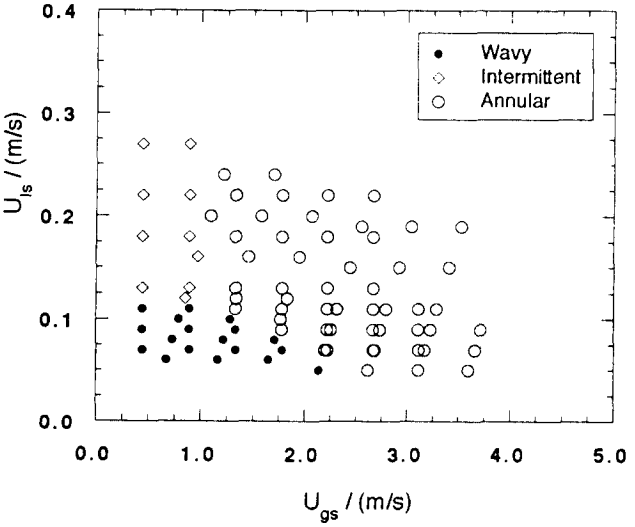

Figure 5. Flow pattern data for convective condensation inside the microfin tube plotted on a U_{gs}-U_{ls} graph.

been more difficult. The flow patterns observed were classified as wavy flow, intermittent flow and annular flow. In some instances (13 data points), we observed an annular flow characterised by a seeming partial dry-out in the upper part of the wall; since we could not assess whether the upper wall was really dry or wetted by a very thin film of liquid, we classified this flow pattern as wavy flow. Fig. 3 also displays the transition frontiers calculated by the flow pattern map proposed by (Weisman et al., 1979). As can be seen, this map correctly identifies 88 of the 96 data points, where the wrong ones are very close to their proper region. We suppose this agreement is also due to the database used to develop the map, that included a refrigerant, i.e., R113. Data were also compared with the flow pattern maps of (Mandhane et al., 1974), of (Taitel and Dukler, 1976) and of (Hashizume, 1983). A near adequate agreement was found only with the last two maps.

Fig. 3 shows the flow pattern data for adiabatic flow in the microfin tube, plotted on a U_{gs}-U_{ls} graph together with the Weisman transition frontiers. It is noteworthy to point out that flow patterns are observed through sight glasses which are not microfinned, but nevertheless they are assumed as fully representatives of the flow regimes actually occurring at the subsection exit. Indeed, we conjecture that the flow structure should experience only a minor disruption in passing to the glass tube, and the flow should not redevelop significantly through the sight glass because of its short length. For the microfin tube, we have data points even at very low values of the superficial vapor velocity, and thus we also observed the plain stratified flow. With respect to the smooth tube, moreover, the annular flow seems characterised by a thinner liquid film, that becomes wavy at low vapor velocities. Finally, with the necessary caution due to the small number of data in the Ugs range between 2 and 3 m/s, microfins do not alterate the transition frontiers toward the annular flow with respect to the smooth tube, while the frontier between the wavy flow and the intermittent flow are slightly shifted upward, i.e., toward higher liquid superficial velocities. Indeed, the Weisman flow pattern map correctly identifies 106 of the 121 data points, while the others fall very close to their region except 6 data for the wavy flow.

In Fig. 4, the flow pattern data for flow boiling inside the microfin tube are plotted on a U_{gs}-U_{ls} graph. The superficial velocities are evaluated by using the thermodynamic quality at the subsection exit. Data here presented refer to quality changes within 0.1-0.2, and to average heat rate ranging from about 6000 to 18000 W/m^2. With respect to the adiabatic flow, we can observe the transition frontiers tend to broaden, and the flow pattern regions result displaced toward higher superficial velocities of the vapor phase. We suppose the frontiers could broaden because most likely flow regimes also depend on the heat rate, while our data are taken for a quite wide range of such values. Regarding the second effect, it is important to point out we are comparing data which are not relative to the same pressure, while flow patterns are affected by this variable. Indeed, a pressure decrement induces a displacement of the flow pattern regions; however, the extent of such a displacement induced by the fluid physical properties variation, as predicted according to (Weiseman et al., 1979) and (Taitel and Duckler, 1976), turns out to be less than that observed. Thus, we infer this effect is mainly due to the heat transfer mechanisms which alterate the arrangement between the liquid and vapor phases with respect to the adiabatic flow. Moreover, the intermittent flow region results also more extended toward higher values of U_{gs} than that for flow boiling inside the smooth tube, not shown here. No comparison is shown for these flow regime data because the authors do not know charts for flow boiling inside microfin tubes, at least with a geometry quite similar to ours. Instead, the flow pattern data for flow boiling inside the smooth tube were compared to the map of (Zhan, 1964) obtaining rather poor results, whereas a comparison to the new flow pattern map

presented by (Steiner, 1993) is still in progress.

Finally, Fig. 5 displays the flow pattern data for convective condensation inside the microfin tube plotted on a U_{gs}-U_{ls} graph. Also these data refer to quality changes within 0.1-0.2. Contrary to what happens for flow boiling, the transition frontier between the intermittent flow and the annular flow results displaced toward lower superficial velocities of the vapor phase, with respect to the adiabatic flow; moreover, the frontier between the annular flow and the wavy flow slightly moves downward, i.e., toward lower liquid superficial velocities. We suppose both the effects are mainly due to the condensation heat transfer mechanisms, even if the pressure effect is not negligibile since data are relevant to moderately different values of pressure. Indeed, the formation of liquid film at the wall favours the onset of the annular flow even at low vapor velocities, whereas the transition from the annular flow to the wavy flow is favoured by the liquid that builds up in the upper part of the wall, when film thickens, and hence tends to flow downward. No comparison is shown either for these data, since there are not flow pattern maps for convective condensation inside microfin tubes to the authors' knowledge. Instead, some flow regime charts are available for condensation inside smooth tubes; a preliminary comparison of our data for this tube with the map of (Tandon et al., 1982) seems to show an adequate agreement.

In Fig. 6 the average boiling heat transfer coefficient h_b is plotted versus the superficial velocities U_{gs}-U_{ls} in order to show its dependence on the flow regimes. For these data, quality change is 0.2 whereas the superficial velocities are evaluated at the average thermodynamic quality over the entire test section $x_m=(x_{in}+x_{out})/2$. The experimental values of h_b are interpolated by a surface that, as can be seen, displays an increasing trend with the superficial velocities; however, the highest increments of h_b occur for increasing values of the vapor velocity, that is during transition between the wavy flow and the annular flow, if liquid velocity is low, or otherwise between the intermittent flow and the annular flow. Hence, as expected, this latter flow regime is characterised by the highest heat transfer coefficients. Finally, we suppose the surface unevenness is most likely due to both experimental and interpolating errors. Obviously, the heat transfer enhancement is penalised by higher pressure drop. Fig. 7 shows these values plotted versus the superficial velocities U_{gs}-U_{ls} together with an interpolating surface. These data are evaluated at the same operative conditions as those of the previous figure. The surface displays a trend quite similar to the surface interpolating heat transfer coefficients; that is pressure drop increases when one passes from the wavy to the intermittent flow and then to the annular flow.

In order to demonstrate clearly the heat transfer coefficient dependence on mass flux, inlet quality and quality change, each of these variables was varied in turn while keeping the others constant. In Fig. 8 the average boiling heat transfer coefficient h_b is plotted versus the mass flux G for the microfin and smooth tubes; such data are for nominal inlet quality x_{in} = 0.3 and for quality change Δx = 0.3. As expected, the boiling coefficient is an increasing function of G; moreover, values for the microfin tube result much higher than those for the smooth one, although they are characterised by a lower growth rate. Indeed, the evaporation enhancement factor, defined as the ratio of heat transfer coefficient of the microfin tube to that of the smooth tube, ranges between about 4 and 1.6 and it is a decreasing function of the mass flux. Instead, the penalty factor, defined as the ratio of pressure drop of the microfin tube to that of the smooth tube, ranges from 1.44 to 1.1 but it is not a strictly decreasing function of mass flux since it displays a maximum at about 130 kg/s m^2, as discussed in (Muzzio et al., 1998). Fig. 9, instead, shows the effect of the average quality x_m on the evaporation heat transfer coefficient for fixed mass flux and quality change (G=224 kg/s m^{-2}, Δx=0.3). For the smooth tube, a slightly marked maximum is observed approximately at x_m = 0.7. It is well established the boiling heat transfer coefficient inside a smooth tube displays a maximum at vapor quality ranging between 0.8 and 0.9, followed by a sharp decrement due to the dryout onset. In the case of average heat transfer coefficients, the averaging process over a quality interval causes a curve flattening and a displacement of the maximum toward lower quality values. For the microfin tube, instead, a continuously increasing trend of the average heat transfer coefficient can be noticed. Hence, we infer this microfin tube provides a dryout shift toward higher qualities in addition to the substantial heat transfer enhancement. Data for the microfin tube were also compared to the predictions of the correlation scheme recently proposed by (Kandlikar and Raykoff, 1996), and of the correlation of (Azer and Sivakumar, 1984) which use the geometric factors proposed by (Carnavos, 1980). The Kandlikar-Raykoff scheme contains three empirical constants that depend on the specific microfin geometry; thus, five different sets of such constants are given for as many microfin geometries but

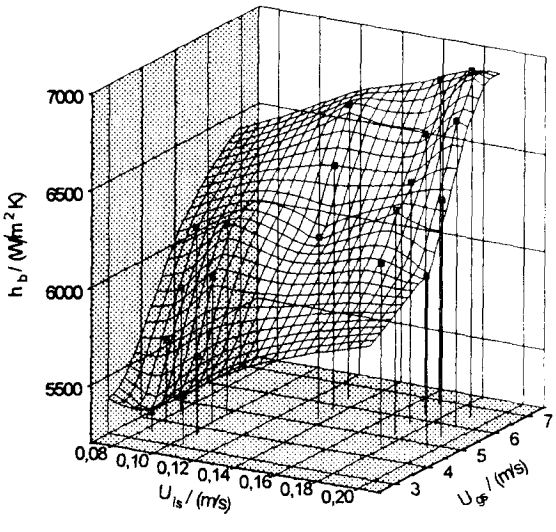

Figure 6. Average boiling heat transfer coefficient for the microfin tube versus the superficial velocities of the liquid and vapor phases for Δx=0.2.

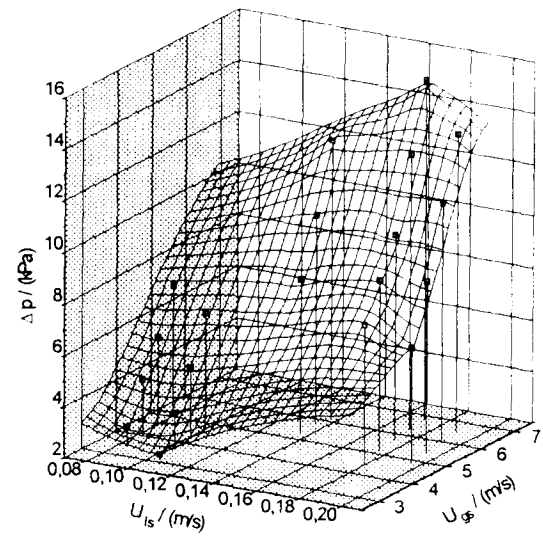

Figure 7. Boiling pressure drop for the microfin tube versus the superficial velocities of the liquid and vapor phases for Δx=0.2.

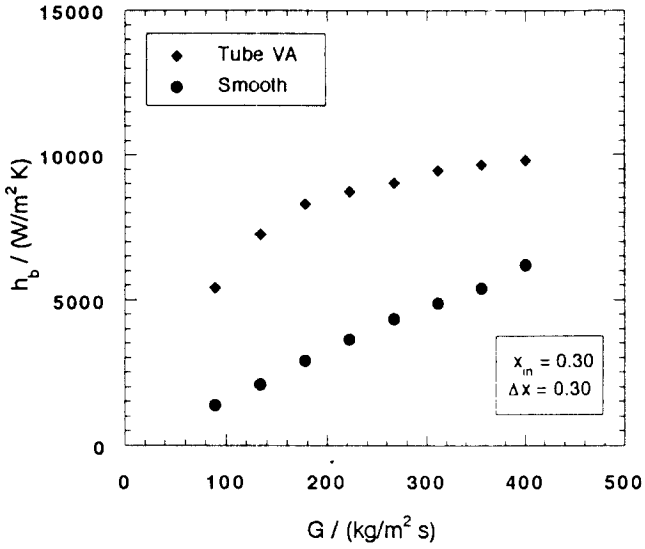

Figure 8. Average boiling heat transfer coefficient plotted versus mass flux for fixed inlet quality and quality change along the test section.

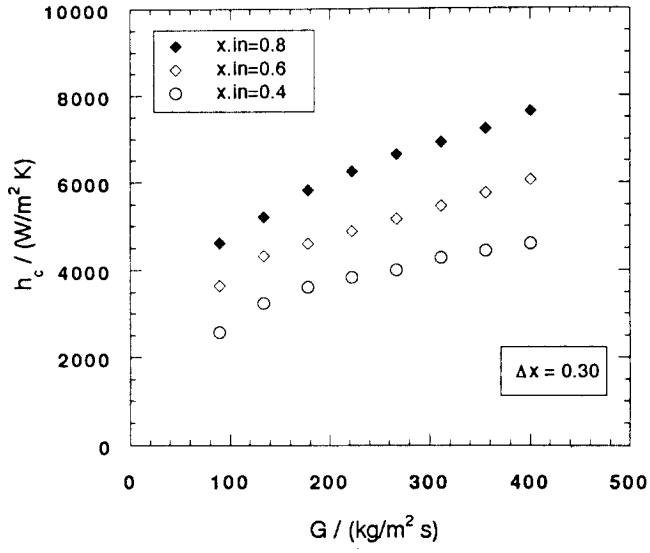

Figure 10. Average condensation heat transfer coefficient for the microfin tube plotted versus mass flux for fixed average quality and for three values of quality change.

none of these is similar enough to our geometry. Consequently, we obtained a rather poor agreement between our data and the Kandlikar-Raykoff predictions which display a trend with xm quite different, as shown in (Muzzio et al., 1998), and deviations up to 33%. The correlation of Azer-Sivakumar underpredicts our data and its trend with G shows a lower growth rate.

Finally, Fig. 10 shows the average condensation heat transfer coefficient h_c for the microfin tube plotted versus the mass flux; such data are for fixed average quality x_m = 0.5 and for three values of the quality change, i.e., Δx equal to 0.6, 0.4 and 0.2, respectively. Data for the smooth tube are also plotted in the same figure for comparison, but only for Δx = 0.6. For the investigated range of G, the all liquid Reynolds number varies from about 3500 to 16000. The heat transfer coefficient is an increasing function of the mass flux as in evaporation, but its dependence on the quality change tends to vanish for values of G higher than 300 kg/s m^2. Fig. 11, instead, shows the condensation heat transfer coefficient for the microfin tube plotted versus the mass flux, for fixed quality change Δx=0.3 and for three values of the inlet quality, i.e., 0.8, 0.6 and 0.4, and hence for three values of the average quality x_m. As can be seen, data display increasing values with x_m for fixed G, whereas their trends with G for fixed x_m are quite similar, i.e., weakly variable values at high G and a higher growth rate at low G. Within the investigated limits of G, the enhancement factor ranges between 2.7 and 1.8 while the penalty factor between 2.1 and 1.2. In addition, condensation heat transfer coefficients for the smooth tube have been compared to the predictions of many correlations. Data result accurately predicted by the correlation of (Cavallini and Zecchin, 1972) and by the scheme of (Paikert, 1988) for G larger than about 240 kg/s m^2, i.e., when the flow regime is annular and hence friction forces prevail over the gravitational ones (this condition has been checked using the criterion reported by Paikert). At lower values of G, instead, the Cavallini-Zecchin correlation does not hold longer while the Paikert scheme tends to overpredict our data with a standard

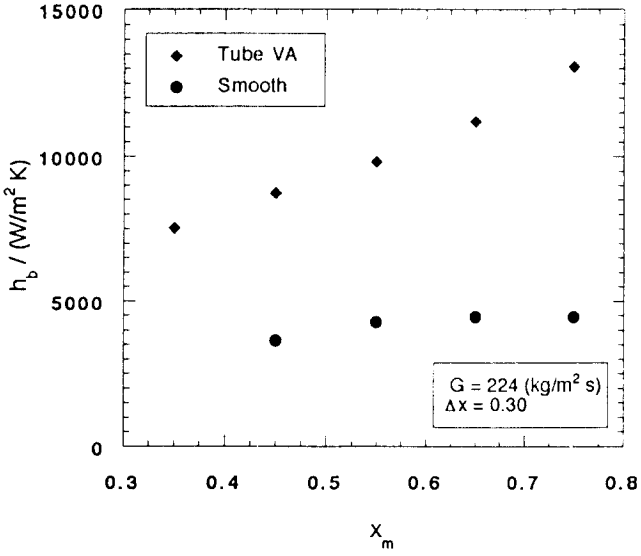

Figure 9. Average boiling heat transfer coefficient plotted versus average quality for fixed mass flux and quality change.

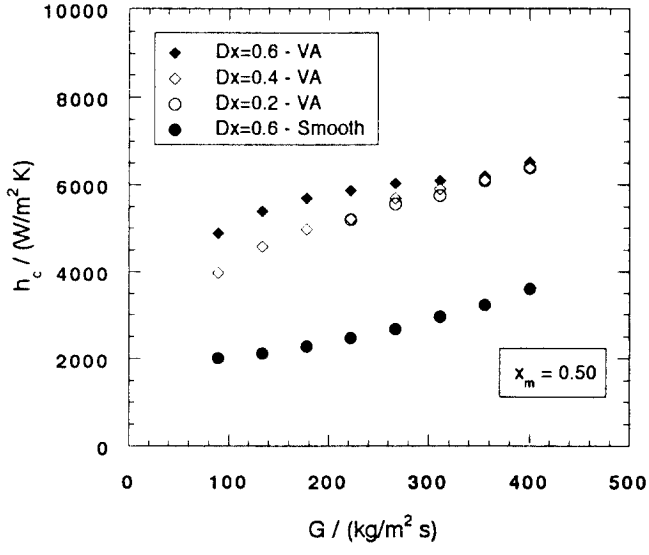

Figure 11. Average condensation heat transfer coefficient plotted versus mass flux for fixed quality change and for three values of average quality.

deviation of about 25%; however, the agreement is greatly improved if a constant of the scheme is empirically corrected. Supported by these results, we compared the data for the microfin tube to the predictions of these two correlations corrected with the geometric factors of Carnavos. The comparison, not displayed here, shows that in many instances these modified correlations do not correctly predict the trend of our data with G, even if the deviation remains within 15% on the average.

CONCLUSIONS

Consideration of flow pattern data brings out the following remarks. In the adiabatic flow, microfins do not seem to affect the transition frontiers toward the annular flow, while the frontier between the wavy and intermittent flow regimes appears shifted toward higher values of the liquid superficial velocity. In flow boiling, the intermittent flow region seems more extended toward higher vapor superficial velocities than that observed in the smooth tube; moreover, the transition frontiers broaden with respect to the adiabatic case because of the variety of heat rate values. In condensation, a displacement of the transition frontier between the intermittent flow and the annular flow is noticed with respect to the adiabatic data, whereas the frontier between the wavy and annular flow regimes slightly moves toward lower liquid superficial velocities. We suppose this frontier displacement is mainly a consequence of the heat transfer, whereas the pressure plays a minor, but not negligibile, role since flow pattern data are taken at moderately different values of pressure. At last, the surfaces interpolating both the heat transfer coefficients and the pressure drops in flow boiling look quite smooth, that is no slope change seemingly occurs at the transition frontiers.

With respect to the smooth tube, the microfin tube tested shows a large heat transfer augmentation with a moderate increment of pressure drop, especially in evaporation where the enhancement factor comes up to 4 and the penalty factor is 1.44 at the most. Finally, the comparison of our heat transfer coefficients to the predictions of some recent correlations, specifically proposed or modified for microfin tubes, shows a rather poor agreement. Indeed, these correlations use empirical constants or geometric factors to account for tube geometry, and therefore by no means they can predict the changes in the flow structure, and eventually in heat transfer mechanisms, induced by new microfin geometries. For the same reason, the data for condensation in annular flow are accurately predicted since correlations are properly applied in their validity range. These conclusions reinforce our conviction that reliable correlations require precise predictions of the local two-phase flow patterns.

NOMENCLATURE

G = mass flux, kg/m^2 s
h = heat transfer coefficient, W/m^2 K
p = pressure, Pa
q = heat flux, W/m^2
T = temperature, K (°C)
U_{ls} = $G(1-x)/\rho_l$ liquid superficial velocity, m/s
U_{gs} = Gx/ρ_g vapor superficial velocity, m/s
x = thermodynamic vapor quality
Δx = change in thermodynamic quality
ρ = density, kg/m^3

Subscripts

b= boiling
c= condensation
g= vapor phase
l = liquid phase
m = mean
r = refrigerant
s = saturation condition
w = wall

ACKNOWLEDGEMENTS

The authors are in debt to Mr. M. Corso of the Politecnico di Milano for the invaluable thecnical assistance in the setting up the apparatus, to Ing. G. Bazzi who helped in performing the experimental runs, and to TREFIMETAUX (France) for supplying the microfin tube. This work is supported by MURST via 60% and 40% grants.

REFERENCES

Azer, N.Z., Sivakumar, V., 1984, Enhancement of saturated boiling heat transfer by internally finned tubes, *ASHRAE Transactions*, Vol. 90, part 1A, pp. 58-73.

Carnavos, T.C., 1960, Heat transfer performance of internally finned tubes in turbulent flow, *Heat Transfer Engineering*, Vol. 1, no. 4, pp.32-37.

Cavallini, A., Zecchin, R., 1972, Scambio termico nella condensazione ad alta velocità di fluidi frigorigeni organici entro tubi: dati sperimentali e correlazioni, (in italian) *La Termotecnica*, Vol. XXVI, no. 4, pp. 199-208.

Hashizume, K., 1983, Flow pattern and void fraction of refrigerant two-phase flow in a horizontal pipe, *Bullettin of JSME*, Vol. 26, no. 219, pp. 1597-1602.

Kandlikar, S.G., Raykoff, T., 1996, Predicting flow boiling heat transfer for refrigerants in microfin tubes, *Proc. of 2nd European Thermal-Sciences and 14th UIT National Heat Transfer Conf.* Vol. 1, pp. 475-482.

Mandhane, J.M., Gregory, G.A., Aziz, K., 1974, A flow pattern map for gas-liquid flow in horizontal pipes, *Int. J. of Multiphase Flow*, Vol. 1, pp. 537-553.

Manwell, Bergles, A.E., 1990, Gas-liquid flow patterns in refrigerant-oil mixtures, *ASHRAE Transactions*, Vol. 96, part 2, pp. 456-464.

Muzzio, A., Niro, A., Arosio, S., 1998, Heat transfer and pressure drop during evaporation and condensation of R22 inside 9.52 mm O.D. microfin tubes of different geometries, *Enhanced Heat Transfer*, in print.

Paikert, P., 1988, Wärmeübertragung bei Kondensation und Bemessung von Verflüssigern, *Handbuch der Kältetechnik*, Springer-Verlag, Berlin, 6ter Band/Teil B.

Steiner, D., 1993, Heat transfer to boiling saturarted liquids, *VDI-Wärmeatlas* , VDI-GCV Verlag, Dusseldorf.

Taitel, Y., Dukler, A.E., 1976, A model for predicting flow regimes transitions in horizontal and near horizontal gas-liquid flow, *AIChE Journal*, Vol. 22, no. 2, pp. 43-55.

Tandon, T.N., Varma, H.K., Gumpta, C.P., 1982, A new flow reggimes map for condensation inside horizonthal tubes", *J. Heat Transfer*, Vol. 104, pp. 763-768.

Thome, J.R., 1994, Two-phase Heat Transfer to New Refrigerants", Heat transfer 1994, *Proc. of 10th Int. Heat Transfer Conference*, Vol. 1, pp. 19-41.

Webb, R.L. 1994, *Principles of enhanced heat transfer*, pp. 446-450, John Wiley & Sons, New York.

Weisman, J., Duncan, D.Gibson, T., Crawford, 1979, Effects of fluid properties and pipe-diameter on two-phase flow patterns in horizontal lines, *Int. J. of Multiphase Flow*, Vol. 5, pp. 437-462.

Zahn, W.R., 1964, A visual study of two-phase flow while evapoarting in horizontal tubes, *J. of Heat Transfer*, Vol. 86, pp. 417-429.

Zürcher, O. Thome, J.R., Favrat, D., 1997, Prediction of two-phase flow patterns for evaporation of refrigerant R-407C inside horizontal tubes, *Convective Flow and Pool Boiling 2nd Conference*, Paper VII-4.